LARGE-EDDY SIMULATION OF A PARTICLE-LADEN TURBULENT CHANNEL FLOW

A.W. Vreman[1], B.J. Geurts[1], N.G. Deen[2] and J.A.M. Kuipers[2]
[1] *Numerical Analysis and Computational Mechanics, Faculty EWI*
[2] *Fundamentals of Chemical Reaction Engineering Group, Faculty TNW*
University of Twente, P.O. Box 217
7500 AE Enschede, The Netherlands
a.w.vreman@utwente.nl

Abstract Large-eddy simulations of a vertical turbulent channel flow with 420,000 solid particles are performed in order to get insight into fundamental aspects of a riser flow. The question is addressed whether collisions between particles are important for the flow statistics. The turbulent channel flow corresponds to a particle volume fraction of 0.013 and a mass load ratio of 18, values that are relatively high compared to recent literature on large-eddy simulation of two-phase flows. In order to simulate this flow, we present a formulation of the equations for compressible flow in a porous medium including particle forces. These equations are solved with LES using a Taylor approximation of the dynamic subgrid-model. The results show that due to particle-fluid interactions the boundary layer becomes thinner, leading to a higher skin-friction coefficient. Important effects of the particle collisions are also observed, on the mean fluid profile, but even more on particle properties. The collisions cause a less uniform particle concentration and considerably flatten the mean solids velocity profile.

Keywords: Large-eddy simulation, turbulence, two-phase flow

1. Introduction

A vertical turbulent channel flow with solid particles is simulated in order to model a section of a riser flow. The turbulent riser is often an industrial environment for important chemical processes, for example the catalytic cracking of oil. Detailed simulations may considerably increase our understanding of the physical dynamics of riser flows, which is required because the scale-up of these flows is very complicated. More knowledge about the formation of clusters of solid particles in these flows may eventually lead to more efficient industrial processes.

Vertical gas-solid flows have been studied experimentally (e.g. Kulick et al. 1994; Nieuwland 1995) and with simulations. Simulations can be performed using a two-fluid model in which the solid phase is modelled as a fluid using continuous variables (e.g., Nieuwland 1995). This approach is subject to relatively many modelling assumptions. A more accurate approach is to conduct simulations with a Langrangian tracking of the motion of each individual particle (Hoomans et al. 1996), where the forces between the fluid and each particle are modelled with a drag law.

Recently the latter technique has been combined with DNS/LES of the fluid flow. Direct numerical simulation (DNS) solves all turbulent scales in the flow, whereas large-eddy simulation (LES) solves the large-scales and models the effect of the small scales with a subgrid-model. These techniques are able to give proper detailed descriptions of the turbulence in a channel flow. LES/DNS of channel flows with solid particles have been performed before (Yamamoto et al. 2001, Squires and Simonin 2002, Portela et al. 2002, Marchioli et al. 2003), but the total volume fraction of particles in these studies remains rather small (0.01 percent) and not all of these works include particle collisions and particle-fluid interactions.

The purpose of this paper is to present LES of a channel flow in which the particle volume concentration is much higher (1.3 percent), in order to study a case which is closer to industrial applications. The simulations are four-way coupled, which means that both particle-fluid and particle-particle interactions (collisions) are included. The discrete particle module developed by Hoomans et al. (1996) is used, in which the spherical particles have a finite size and all (inelastic) collisions are taken into account. The LES-equations of the gas-phase are closed with an approximation of the dynamic subgrid-model.

In order to study both the effect of the particle collisions and the effects of the particle-fluid interactions we compare the following three simulations: (1) a turbulent channel flow without particles, (2) a turbulent channel flow with particles, but without collisions (two-way coupled case) and (3) a turbulent channel flow with colliding particles (four-way coupled case). The differences between cases 1 and 2 quantify the effects of the particle-fluid interactions and the differences between cases 2 and 3 quantify the effects of the particle collisions.

2. The equations for gas-solid channel flow

Description of the gas phase

The Navier-Stokes equations that govern a compressible flow in a porous medium read:

$$\partial_t(\rho\epsilon) + \partial_j(\rho\epsilon u_j) = 0, \quad (1)$$

$$\partial_t(\rho\epsilon u_i) + \partial_j(\rho\epsilon u_i u_j) = -\partial_i(\epsilon p) + \partial_j \epsilon\sigma_{ij} + (\rho\epsilon g + \epsilon p_g)\delta_{i3} + f_i, \quad (2)$$

$$\partial_t(\epsilon e) + \partial_j((e+p)\epsilon u_j) = \partial_j(\epsilon\sigma_{ij}u_i) + (\rho\epsilon g + \epsilon p_g)u_3 + f_i u_i - \partial_j(\epsilon q_j) \quad (3)$$

where the symbols ∂_t and ∂_j denote the partial differential operators $\partial/\partial t$ and $\partial/\partial x_j$ respectively.

The coordinate x_3 denotes the streamwise direction of the channel flow, x_2 is the normal and x_1 is the spanwise direction. The domain is rectangular and the channel width, height and depth equal $L_2 = 0.05m$, $L_3 = 0.30m$ and $L_1 = 0.075m$ respectively. No-slip boundary conditions are imposed in the x_2-direction and periodic boundary conditions are assumed for the stream- and spanwise directions. Furthermore, ρ is the density, ϵ is the porosity, $\mathbf{u}$ the velocity, p the pressure and $e = p/(\gamma-1) + \frac{1}{2}\rho u_k u_k K$ the total energy per volume unit. The constant γ denotes the ratio of specific heats $C_P/C_V = 1.4$.

The viscous stress σ_{ij} is defined as the product of viscosity $\mu = 3.47 \cdot 10^{-5} kg/(ms)$ and strain-rate

$$S_{ij}(u) = \partial_i u_j + \partial_j u_i - \tfrac{2}{3}\delta_{ij}\partial_k u_k. \quad (4)$$

The heat-flux q_j is defined as $-\kappa\partial_j T$ where T is the temperature and $\kappa = 0.035W/(mK)$ the heat-conductivity coefficient.

Pressure, density and temperature are related to each other by the equation of state for an ideal gas $\rho RT = M_{gas}p$, where $R = 8.314J/(molK)$ is the universal gas constant and M_{gas} =$0.0288kg/mol$ is the mass of the gas per mol. The gravitation accelaration equals $g = -9.81m/s^2$, p_g is an external pressure gradient and the symbol f_i denotes the force of the particles on the flow per volume unit.

The equations formulated above are equivalent to the equations governing a compressible ideal gas with velocity $\mathbf{u}$, temperature T, density $\rho^c = \epsilon\rho$, pressure $p^c = \epsilon p$, viscosity $\mu^c = \epsilon\mu$ and heat-conductivity $\kappa^c = \epsilon\kappa$. Therefore to solve this flow it is convenient to use a standard compressible code with an addition of the forcing terms representing gravitation and the forces from the particles on the fluid.

We are interested in a section of a riser flow with a vertical velocity of about $4m/s$. The parameters of the fluid in the riser are close to those for air. The initial fluid density equals ρ_1 =$1.0kg/m^3$. With a normal value of the initial pressure (around $10^5 N/m^2$) the flow has a very low Mach number around 0.01, which is extremely expensive to simulate with a compressible solver. Therefore we use a much lower pressure ($340N/m^2$) which results in a Mach number of appromixately 0.2. At this Mach number the turbulent channel flow can still be regarded as incompressible, i.e. a further reduction of the Mach number does not significantly change the turbulent statistics, including pressure fluctuations.

The flow is driven by the pressure gradient p_g, which is a function of time only and its level is such that the total fluid mass flow is constant. For a channel

flow without particles the value of p_g corresponds to $\tau_w = 0.0625N/m^2$, $u_\tau = 0.25m/s$ and $Re_\tau = 180$.

Description of the solids phase

The discrete particle model is a hard sphere collision model. It calculates the motion of particles in the fluid and includes the particle collisions with a general restitution coefficient of 0.97, a tangential restitution coefficient of 0.33 and friction coefficient of 0.1. The forces on a particle that are taken into account are gravitation, pressure and the drag force resulting from the velocity difference with the surrounding fluid. The Ergun and Wen & Yu drag law is used, which is precisely described in Hoomans et al. (1996). The mean velocity of the riser is low enough to neglect the heat transfer during particle collisions and the heat transfer between particles and fluid. The particle diameter equals $0.4mm$ and the particle density equals ρ_2 $=1500kg/m^3$. The number of particles equals $N_p = 419904$. With the parameters above the average volume fraction of the particles equals 0.013. The Stokes-response time equals $0.4s$.

Description of the numerical method

The equations for the fluid phase are solved with a second-order finite volume method on a collocated grid. The equations are discretized in the divergence form as described by equations (1-3). The control volume of the convective and pressure terms equals eight grid-cells. Control volumes of one cell are used to discretize the derivatives that are required for the viscous/subgrid-fluxes and for the divergences of these fluxes. The integrations over cell-faces are all performed with the trapezoidal rule.

The grid contains $N_1 \times N_2 \times N_3$ cells and is only non-uniform in the normal direction. The simulations presented in the following are performed on a grid with $N_1 = 32$ and $N_2 = N_3 = 64$. The first grid point $x_{2,1} = 0.2mm$ in the normal direction corresponds with $y^+ = 1.5$. The porosity parameter ϵ is determined by counting the particles within each cell of an auxiliary grid, which is uniform and contains $32 \times 25 \times 64$ cells, chosen such that in each direction the mesh-spacing of this grid is considerably larger than the particle diameter (Hoomans et al 1996). Linear interpolation routines communicate the information from grid-nodes to particle positions and vice-versa.

The discretization in time is explicit: a second-order Runge-Kutta method for the fluid phase and Euler for the particles. The time step equals $2 \cdot 10^{-5}s$ for the fluid phase and $10^{-4}s$ for the solids phase. The simulations run until at least $t = 5s$, while statistics are accumulated between $t = 3s$ and $t = 5s$.

3. Subgrid-modeling

The equations governing the fluid phase are solved by means of LES, which implies that a 'bar'-filter is applied to the equations (1-3), with filter width Δ_i

in the x_i-direction taken equal to the grid-spacing. The filtered equations are similar to equations (1-3), with the difference that in the left-hand side of the momentum equation a subgrid-stress is included, $\partial_j \tau_{ij}$ with

$$\tau_{ij} = \overline{\rho\epsilon u_i u_j} - \overline{\rho\epsilon u}_i \overline{\rho\epsilon u}_j / \overline{\rho\epsilon}. \tag{5}$$

For a full presentation of the filtered equations for compressible flow we refer to Vreman et al. (1995). The dynamic model (Germano et al. 1991) for τ_{ij} is based on the Smagorinsky eddy-viscosity

$$m_{ij} = -c_S \overline{\rho\epsilon} \Delta^2 S(\tilde{u}) S_{ij}(\tilde{u}), \quad S = (\tfrac{1}{2} S_{ij} S_{ij})^{\frac{1}{2}}, \quad \Delta = (\Delta_1 \Delta_2 \Delta_3)^{\frac{1}{3}}, \tag{6}$$

where $\tilde{u}_i = \overline{\rho\epsilon u_j} / \overline{\rho\epsilon}$, a sort of Favre-filter for compressible flows with porosity. The dynamic procedure employs an extra filter with a larger filter width $\hat{\Delta} = 2\Delta$, and the dynamic coefficient c_S is computed by

$$c_S = \frac{< M_{ij} L_{ij} >}{< M_{ij} M_{ij} >}, \tag{7}$$

where $< . >$ denoted an average over the homogeneous directions in the channel and

$$L_{ij} = \widehat{[\overline{\rho\epsilon} \tilde{u}_i \tilde{u}_j]} - \widehat{\overline{\rho\epsilon u}_i} \widehat{\overline{\rho\epsilon u}_j} / \widehat{\overline{\rho\epsilon}}, \tag{8}$$

$$M_{ij} = -\widehat{\overline{\rho\epsilon}} (\sqrt{5}\Delta)^2 S(\widehat{\overline{\rho\epsilon u}} / \widehat{\overline{\rho\epsilon}}) S_{ij}(\widehat{\overline{\rho\epsilon u}} / \widehat{\overline{\rho\epsilon}}) + \widehat{[\overline{\rho\epsilon} \Delta^2 S(\tilde{u}) S_{ij}(\tilde{u})]}. \tag{9}$$

The notation $\widehat{[.]}$ indicates that the hat-filter is applied to the expression between the brackets. The factor $\sqrt{5}$ is related to the choice of top-hat filters and a ratio of 2 between test-filter and basic filter (Vreman et al. 1997).

Next we simplify the dynamic model in line with the approaches described by Pope (2000, p. 623) and Chester et al. (2001). Thus, in the following Taylor expansions are used to approximate the tensors L_{ij} and M_{ij}. In this paper, only the $O(\Delta^2)$ terms are taken into account. For the tensor L_{ij} this results in an expression similar to the gradient model,

$$L_{ij} = \tfrac{1}{3} \overline{\rho\epsilon} \Delta_k^2 \partial_k \tilde{u}_i \partial_k \tilde{u}_j. \tag{10}$$

For the simplification of M_{ij} we use that $\hat{w} = \bar{w} + O(\Delta^2)$, which yields

$$M_{ij} = -4 \overline{\rho\epsilon} \Delta^2 S(\tilde{u}) S_{ij}(\tilde{u}). \tag{11}$$

The dynamic coefficient is again obtained with equation (8). Thus the simplified procedure for c_S, with simplified L_{ij} and M_{ij}, does not need explicit test-filtering. The resulting coefficient essentially equals the dissipation of the eddy-viscosity model to the dissipation of the gradient model.

The computations presented in this paper have been performed with this approximated dynamic model (equations (6-7,10-11)), which is is much cheaper to evaluate than the standard dynamic model. Simulations with other subgrid-models are currently performed, for example with the standard dynamic model (using equations (8-9)) and with a multiscale subgrid-model (Vreman 2003).

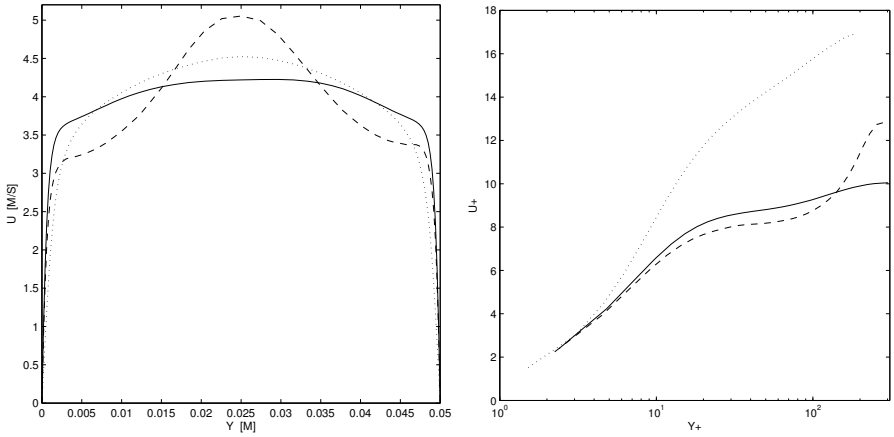

Figure 1. Dimensional (left) and non-dimensional (right) mean streamwise fluid velocity $\langle u_z \rangle$. Simulation with colliding particles (solid), with non-colliding particles (dashed) and without particles (dotted).

4. Results

Results of the simulations are shown in figures 1-3. A comparison between the case without and the cases with particles in figure 1 shows that due to particle-fluid interactions the boundary layer becomes thinner (figure 1a) leading to a higher skin-friction coefficient (figure 1b). We also observe important effects of the collisions, on the mean fluid velocity profile (figure 1), but even more on particle properties (figures 2-3). The mean particle velocity with collisions is flatter than without collisions (figure 2a). We also observe that the near-wall particle velocity is positive and does not drop to zero. This is in agreement with the observation that the mean fluid velocity profile in the boundary layer is enhanced by the forces of the particles on the fluid.

Comparison of the cases with and without collisions shows that the collisions cause a less uniform particle concentration, as demonstrated by figures 2b-3. An increase of the particle concentration near the walls is only observed for the case that includes collisions (figure 2b). Although significant, the increase remains rather small, which is attributed to the fact that the particles are coarse. The near-wall effect was observed to be much stronger in a more diluted simulation using finer particles ($d_p = 0.04mm$) and a volume concentration of $1.3 \cdot 10^{-5}$. Figure 3a shows that the case with collisions contains relatively dense regions of particles, which are upward transported by the mean velocity. Without collisions these regions are considerably smaller and less dense (figure 3b), and thus it may be concluded that the particle-particle interactions play a crucial role in the formation of dense regions of particles.

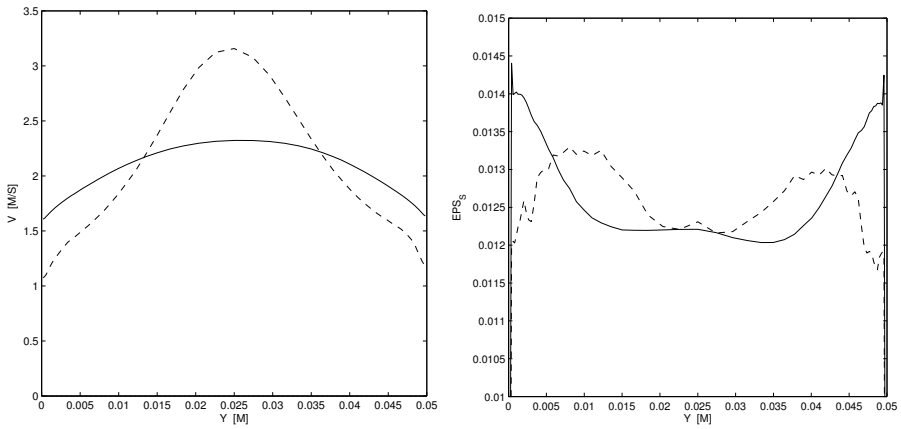

Figure 2. Mean streamwise particle velocity $\langle v_z \rangle$ (left) and mean volume fraction of the particles $\langle \epsilon_s \rangle$ (right). Simulation with colliding particles (solid) and with non-colliding particles (dashed).

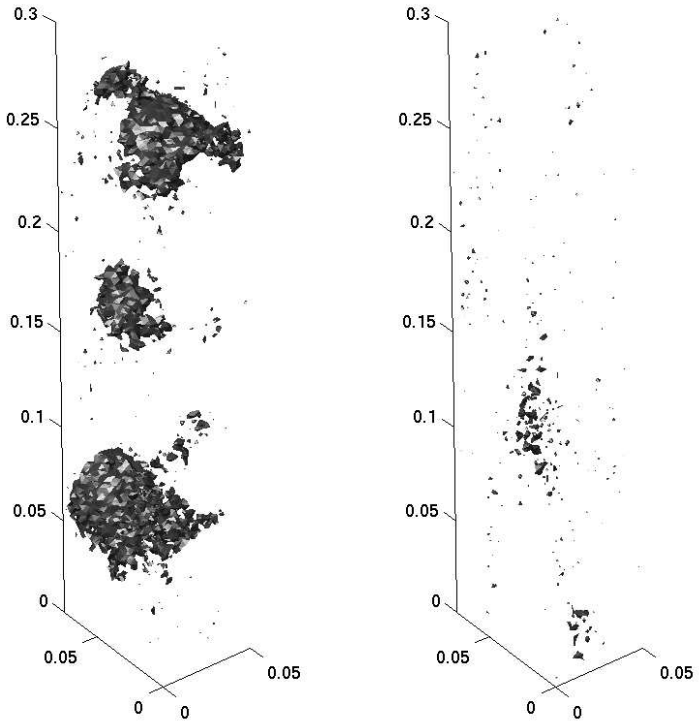

Figure 3. Isosurfaces $\epsilon_s = 0.03$ at $t = 3s$ with collisions (left) and without collisions (right).

We conclude therefore that particle-fluid forces and collisions between particles strongly alter important properties of both phases. This indicates the necessity of a full four-way coupled model for detailed simulations of such flows.

Acknowledgements

A.W. Vreman is grateful to J.G.M. Kuerten for useful discussions on this topic and to J.M. Link for assistance with the discrete particle model. The initial conditions for turbulent channel flow were provided by N.D. Sandham. The computations were performed through grant NCF SC-144.

References

Chester, S., Charlette, F., and Meneveau, C. (2001). "Dynamic model for LES without test filtering: Quantifying the accuracy of Taylor series approximations", Theor. Comp. Fluid Dyn. 15, 165-181.

Germano, M., Piomelli, U., Moin, P., and Cabot, W.H. (1991). "A dynamic subgrid-scale model", Phys. Fluids A 3, 1760-1765.

Hoomans, B.P.B., Kuipers, J.A.M., Briels, W.J., and van Swaaij, W.P.M. (1996). "Discrete particle simulation of bubble and slug formation in a two-dimensional gas-fluidised bed: A hard-sphere approach", Chem. Eng. Science 51, 99-118.

Kulick, J.D., Fessler, J.R., and Eaton, J.K. (1994). "Particle response and turbulence modification in fully developed channel flow", J. Fluid Mech. 227, 109-134.

Marchioli, C., Giusti, A., Salvetti, M.V., and Soldati, A. (2003). "Direct numerical simulation of particle wall transfer and deposition in upward turbulent pipe flow", Int. J. of Multiphase Flow 29, 1017-1038.

Nieuwland, J.J. (1995). "Hydrodynamic modelling of gas-solid two-phase flows", PhD-Thesis, University of Twente.

Pope, S.B. (2000), "Turbulent flows", Cambridge University Press.

Portela, L.M., Ferrand, V., Bijlard, M.J., and Oliemans, R.V.A. (2002). "Effect of the turbulence-dynamics modification on turbulence models for particle-laden wall-bounded flows", Proceedings of the 10th workshop on two-phase flow predictions, Merseburg, 152-163.

Squires, K.D., and Simonin, O. (2002). "Recent advances and perspective of DNS and LES for dispersed two-phase flow", Proceedings of the 10th workshop on two-phase flow predictions, Merseburg, 152-163.

Vreman, A.W. (2003). "The filtering analog of the variational multiscale method in large-eddy simulation", Phys. Fluids, to appear in the September issue.

Vreman, B., Geurts, B.J., and Kuerten, J.G.M. (1995), "A priori tests of large-eddy simulation of the compressible plane mixing layer", J. Eng. Math. 29, 299-237.

Vreman, B., Geurts, B.J., and Kuerten, J.G.M. (1997). "Large-eddy simulation of the turbulent mixing layer", J. Fluid Mech. 339, 357-390.

Yamamoto, Y., Potthoff, M., Tanaka, T. Kajishima, T., and Tsuji, Y. (2001). "Large-eddy simulation of turbulent gas-particle flow in a vertical channel: effect of considering inter-particle collisions", J. Fluid Mech. 442, 303-334 (2001).